ELSEVIER

Journal of Alloys and Compounds 321 (2001) 261–266

Journal of ALLOYS AND COMPOUNDS

www.elsevier.com/locate/jallcom

High-temperature electrochemical study of $Na_2O–MoO_3$ melts

Ray Y. Lin*, John F. Elliott[1]

Department of Materials Science and Engineering, M.L. 0012, University of Cincinnati, Cincinnati, OH 45221, USA

Received 5 September 2000; accepted 5 December 2000

Abstract

Physical chemistry of the $Na_2O–MoO_3$ system was investigated using a high-temperature electrochemical cell with Na, β-alumina as the solid electrolyte. The reference electrode was a solid mixture of tungsten, tungsten sulfide and sodium sulfide. The cell may be expressed as the following:

$$\begin{array}{l|l|l} W(s), WS_2(s) & Na^{+} & O_2(g), Pt(s) \\ Na_2S(s) & \beta\text{-alumina} & Na_2O–MoO_3 \text{ melt} \end{array}$$

The activity of Na_2O in the $Na_2O–MoO_3$ melt in the composition range from 50.87 to 92.18 mol% MoO_3 and temperatures from 890 to 1230 K was determined using this cell. Partial molar enthalpies of mixing for Na_2O in the melt were evaluated from the temperature dependence of the activity data using the Gibbs–Helmhotz equation. The values agree with those reported in the literature from calorimetric measurements. The activity of MoO_3 in the melt as a function of the melt composition at various temperatures was also determined using the Gibbs–Duhem equation and the $Na_2O–MoO_3$ phase diagram. © 2001 Elsevier Science B.V. All rights reserved.

Keywords: Thermochemistry; $Na_2O–MoO_3$ system; High temperature EMF cells; Enthalpy; Hot corrosion

1. Introduction

Like tungsten, molybdenum is used in high-temperature alloys to increase their ductility. Typical examples are: nickel-based Udimet-500 with 4% Mo, B-1900 with 6.0% Mo, U-700 with 4.4% Mo, Waspaloy with 4.25% Mo, and IN-738 with 1.75% Mo. As these alloys are exposed to high-temperature oxidizing environments, oxides of Mo form along with other oxides. In the presence of hot corrosion media such as molten sodium sulfate [1–3], WO_3 or MoO_3 and Na_2O may combine to form low-melting-point salts [4–7] and result in accelerated corrosion. To understand the mechanism of hot corrosion of this type of material, physical chemistry of the related oxide salt systems must be studied.

Limited investigations have been devoted to the mixed oxide system between MoO_3 and Na_2O. The phase diagram of the $Na_2O–MoO_3$ system was determined by Hoermann [8] and more completely by Caillet [9] using a differential thermal analysis technique. Koehler et al. [10] determined the heats of formation of $Na_2MoO_4(s)$ and $Na_2Mo_2O_7(s)$ at 298 K by the calorimetric method. The heat capacities and entropies of $Na_2MoO_4(s)$ at temperatures between 52.67 and 296.35 K have also been measured by Weller and King [11]. Navrotsky and Kleppa [12] determined enthalpies of solution of $MoO_3(s)$ and $Na_2MoO_4(l)$ in the $Na_2O–MoO_3$ melt at 970 K with a high-temperature calorimeter. For high temperature calorimetric studies, high temperature solvent selection is one of the most critical challenges in the success of the experiment. Kleppa and co-workers have experimented with a number of different solvents including sodium molybdates [13–16]. However, no information on the Gibbs free energies of the $Na_2O–MoO_3$ system is available. As a continuing effort in investigating physical chemistry of molten salts containing Na_2O, this study reports the investigation of the $Na_2O–MoO_3$ system applying a high temperature electromotive force (EMF) cell. Other systems reported previously include the $Na_2O–WO_3$ and $Na_2O–P_2O_5$ systems [18,19].

---

*Corresponding author. Tel.: +1-513-5563-116; fax: +1-513-5562-569.

E-mail address: ray.lin@uc.edu (R.Y. Lin).

[1] Previously with the Department of Materials Science and Engineering, Massachusetts Institute of Technology, Cambridge, MA 02139, USA.

0925-8388/01/$ – see front matter © 2001 Elsevier Science B.V. All rights reserved.
PII: S0925-8388(01)00958-6

2. Experimental

2.1. The cell

The electrochemical cell employed in the present study utilized a Na, β-alumina solid electrolyte:

$$\begin{array}{l|l|l} \mathrm{W(s), WS_2(s)} & \mathrm{Na^+} & \mathrm{O_2(g), Pt(s)} \\ \mathrm{Na_2S(s)} & \beta\text{-alumina} & \mathrm{Na_2O{-}MoO_3\ melt} \end{array}$$

This type of cell has been used in earlier investigations [17–20]. A schematic diagram of the cell is shown in Fig. 1. The electrode reactions are: at the anode:

$$1/2\mathrm{W(s)} + \mathrm{Na_2S(s)} = 1/2\mathrm{WS_2(s)} + 2\mathrm{Na^+} + 2\mathrm{e^-} \tag{1}$$

and at the cathode:

$$2\mathrm{Na^+} + 2\mathrm{e^-} + 1/2\mathrm{O_2(g)} = (\mathrm{Na_2O})_{\text{in the melt}} \tag{2}$$

The overall cell reaction is:

$$1/2\mathrm{W(s)} + \mathrm{Na_2S(s)} + 1/2\mathrm{O_2(g)} = 1/2\mathrm{WS_2(s)} + (\mathrm{Na_2O})_{\text{in the melt}} \tag{3}$$

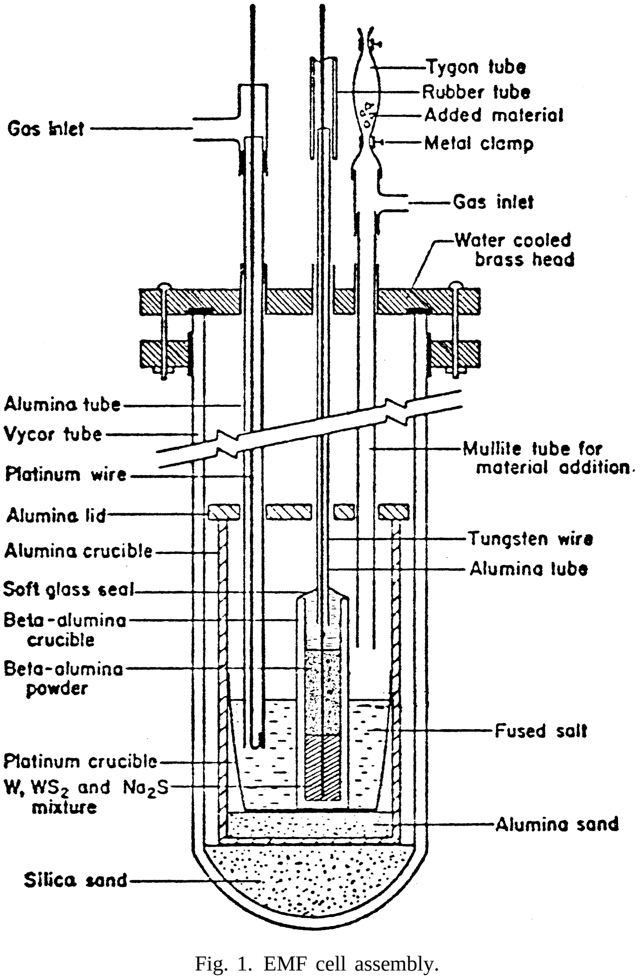

Fig. 1. EMF cell assembly.

and the Nernst equation is:

$$E = E^0 - \frac{RT}{2F} \cdot \ln \frac{a_{\mathrm{Na_2O}} a_{\mathrm{WS_2}}^{1/2}}{a_{\mathrm{W}}^{1/2} a_{\mathrm{Na_2S}} P_{\mathrm{O_2}}^{1/2}} \tag{4}$$

where E is the cell potential; E^0 is the standard cell potential; R is the universal gas constant; T is the the cell temperature in K; F is the Faraday constant, or 96 487 coulomb/equiv. and a_i values are activities of components i. During the experiment the oxygen partial pressure at the cathode was fixed at either 0.05 or 0.21 atm (1 atm = 101 325 Pa).

The standard cell potential was calculated from:

$$E^0 = -\Delta G_3^0/2F \tag{5}$$

where ΔG_3^0 is the standard Gibbs free energy for Eq. (3) and can be calculated as:

$$\Delta G_3^0 = 1/2\Delta G_{\mathrm{WS_{2(s)}}}^0 + \Delta G_{\mathrm{Na_2O(l)}}^0 - \Delta G_{\mathrm{Na_2S}}^0 \tag{6}$$

The standard free energies of the compounds are obtained from the JANAF Tables [21] and from the work of Hager and Elliott [22] for tungsten sulfide. The standard states for all substances used in this study are pure solid W, Na_2S and WS_2, pure oxygen at 1 atm and pure liquid Na_2O, respectively. All experiments in this study were carried out at temperatures between 890 and 1230 K, which are well below the melting points of all substances at the anode. Thus, Eq. (4) can be reduced to:

$$E = E^0 - \frac{RT}{2F} \cdot \ln (a_{\mathrm{Na_2O}}/P_{\mathrm{O_2}}^{1/2}) \tag{7}$$

The value of ΔG_3^0 has been calculated to be:

$$\Delta G_3^0 = -100\,180 + 50.44T\ \mathrm{kJ} \tag{8}$$

and Eq. (7) becomes:

$$\log a_{\mathrm{Na_2O}} = 1/2 \log P_{\mathrm{O_2}} - 2.63 - (10\,080E - 5233)/T \tag{9}$$

2.2. The materials

The schematic drawing of the cell used in this study is shown in Fig. 1. This cell is similar to the EMF cell used previously by Lin and Elliott [18]. The material in the anode chamber was a powder mixture of W(s), WS_2(s), and Na_2S(s) in a ratio of 1:1:4 (w/w). They were mixed and ground with a mortar and pestle in a glove bag filled with dried argon. The powder mixture was prepared and stored in a desiccator for subsequent uses. The lead wire in the anode is pure tungsten wire of 762 μm in diameter. The electrolyte is solid Na, β-aluminum crucible. The preparation procedure of this solid electrolyte crucible has been reported in detail before [20]. In the cathode, the Na_2O–MoO_3 molten salt was contained in a platinum crucible (3 cm height×3 cm diameter). The composition of the charging material at the cathode was determined by weighing fixed amounts of dried MoO_3(s) and Na_2MoO_4(s). These materials were obtained by heating the respective powders in vacuum at 200°C for 24 h for drying, compacted into pellets, cracked into small chips and stored in a desiccator for subsequent uses. During each run, the composition of the cathode melt was varied by adding MoO_3(s) chips or dried Na_2O(s) particles via a quartz tube as indicated in Fig. 1. Pure oxygen was bubbled through the melt via a single bore alumina tube at approximately 0.5 cm below the surface of the melt. Bubbling of oxygen also served as a stirring mechanism in the melt to minimize the composition gradient throughout the cathode. The lead wire at the cathode was platinum. To get stable EMF readings, the platinum wire was wrapped around the exterior surface of the Na, β-alumina crucible in the melt and touched the platinum crucible.

2.3. Measurements

The cell potential was measured with a Beckman pH meter with an internal impedance of 10^9 Ohm. Steady cell potentials were observed during each experiment. Typically electromotive force (EMF) readings became constant after the cell temperature reached the preset value or after each component addition to the melt for getting a new cathode melt composition. Since the cathode lead wire is platinum and the anode lead wire is tungsten, the cell potential must be corrected for the junction potential of the W/Pt junction. That potential was found to follow the linear relationship of:

$$E_{W/Pt} = 23.5 - 0.0395T\ (\pm 0.2)\ \mathrm{mV} \qquad (10)$$

The cell temperature was obtained by means of a calibrated Pt/Pt–10% Rh thermocouple and a Rubicon potentiometer regularly and at the time an EMF reading was taken. The thermocouple was protected by an alumina sheath and its tip was placed within 5 mm of the cathode melt surface. From the calibrated furnace temperature profile, it was estimated that the true cell temperature was within ±1°C of the measured value. For each cell, after an initial period of approximately 5 h for cell stabilization, satisfactory readings were obtained within 90 min after a new temperature was set from the controller. The cell potential also responded very quickly after a component addition to the cathode melt. EMF readings were continuously recorded and the equilibrium EMF value was taken to be the reading when there was no more than ±0.1% variation in the measured EMF over a 60-min period.

The reproducibility of the cell was verified by repeating the experimental conditions through (a) changing the experimental temperature or (b) changing the melt composition by adding dried MoO_3 or Na_2O into the cathode. On the other hand, the cell reversibility was certified by polarizing the cell with a 50 mA current through the cathode and a working electrode and observing the cell potential recovery after the polarizing current was terminated. The cell polarization was carried out both cathodically and anodically. Results of the polarization test showed that all cell potentials returned to the initial readings within 60 min indicating that there were no other reactions occurring during polarization and that the cells were reversible.

3. Results and discussion

3.1. Experimental data

A total of 22 cells were established to conduct the present investigation. Each cell was used to generate multiple experimental data by alternating the cell temperature or by adding dried pellets of Na_2O or MoO_3 to change the cathode melt composition. Most cells performed well. A few cells failed as evidenced by continuous drifting of the EMF readings. Cells with drifting EMF readings were found to have improper glass seal which resulted in the oxidation of the materials in the anode. Fig. 2 shows the measured activity of Na_2O in the melt as a function of the melt composition at 890, 980 and 1200 K. Data in this figure show that the reproducibility of the high temperature EMF cell is very good. The 1200 K measurements were limited to melts with the mole fraction of MoO_3, N_M, being smaller than 0.65. A few experiments were done with N_M greater than 0.65 at 1200 K. It was found that the cell failed rapidly due to the attack of the electrolyte by the highly acidic cathode melt, which was aggressive at elevated temperatures such as 1200 K. Unlike the Na_2O–WO_3 system [18], the activity of Na_2O data in the Na_2O–MoO_3 melt did not vary linearly with the melt composition. The Na_2O activity data at 980 K were fitted into a second-order polynomial function of the melt composition as shown below:

$$\log a_{Na_2O} = -12.367N_M^2 - 3.561N_M - 8.59,\ R^2 = 0.9964 \qquad (11)$$

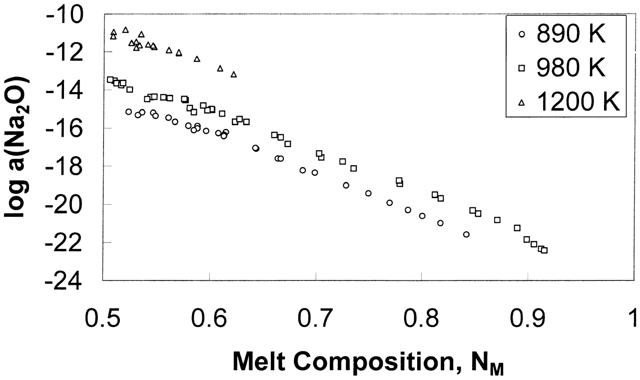

Fig. 2. The activity of Na_2O in the Na_2O–MoO_3 melt.

where N_M is the mole fraction of MoO_3 in the Na_2O–MoO_3 melt. No curve fitting was made for data at 890 and 1200 K due to the limited numbers of measurements. However, as to be shown below, an equation of Na_2O activity for the entire melt region of the Na_2O–MoO_3 system has been developed using the data from the 980 K measurements.

Fig. 3 shows the Na_2O activity as a function of temperature at fixed melt composition with $N_M = 0.51$, 0.53, 0.55 and 0.60. Data in this figure show that the activity of Na_2O at a constant melt composition forms a straight line relationship with $1/T$. Linear regression analysis gives the best fit equation for the data at each composition. Table 1 lists these best-fit equations along with the correlation coefficients. The slope can be used to estimate the enthalpy of solution of $Na_2O(l)$ in the melt as to be discussed below.

The values of the correlation coefficient suggest that the reproducibility of the EMF measurements is very good. It is to be noted that as many as 34 EMF measurements were made to obtain the equation for $N_M = 0.53$.

3.2. Enthalpy of solution

As indicated earlier, Navrotsky and Kleppa [12] had measured the enthalpy of solution of $MoO_3(s)$, $H^M_{M(s)}$, and the enthalpy of solution of $Na_2MoO_4(l)$, H^M_{NM}, in the Na_2O–MoO_3 melts at 970 K using a high-temperature calorimeter. Their data may be used to deduce the enthalpy of solution of $Na_2O(l)$, H^M_N, in the melt by the following two equations if the enthalpy of reaction, H_R, between $Na_2O(l)$ and $MoO_3(l)$ to form $Na_2MoO_4(l)$ as well as the heat of melting of $MoO_3(s)$, $\Delta H_{m,\,MoO_3}$, are available:

$$H^M_{M(s)} = \Delta H_{m,\,MoO_3} + H^M_M \quad (12)$$

$$H^M_N + H^M_M = H_R + H^M_{NM} \quad (13)$$

Table 1
The straight line relationship between log a_{Na_2O} and $1/T$ at various compositions in the Na_2O–MoO_3 melt

N_M	Log a_{Na_2O}	R^2
0.51	$-14\,838/T+1.33$	0.9655
0.53	$-14\,334/T+0.40$	0.988
0.55	$-14\,447/T+0.16$	0.9719
0.60	$-14\,208/T-1.04$	0.9892

From the JANAF Tables [21], at 970 K, the enthalpy of formation of $MoO_3(s)$ and $MoO_3(l)$ are -733.04 and -686.31 kJ/mole, respectively. Thus, $\Delta H_{m,\,MoO_3}$ at 970 K is 46.73 kJ/mole. This value may be used in Eq. (12) to obtain H^M_M from Navrotsky and Kleppa's $H^M_{M(s)}$ measurements. The data may be represented by the following equation:

$$H^M_M = -0.6163N^2_M + 97.835N_M - 89.879,\ \text{kJ/mole} \quad (14)$$

For the H_R value, data on Na_2O and MoO_3 might be retrieved from the JANAF Tables [21] or other sources. However, there is no enthalpy data in the JANAF Tables on Na_2MoO_4. Kubaschewski and Alcock [23] cited enthalpies of transformation for Na_2MoO_4 as well as heat of formation and standard entropy of $Na_2MoO_4(s)$ at 298 K. But no heat capacity data were given.

Alternatively, the enthalpy of reaction between $Na_2O(l)$ and $MoO_3(l)$ to form $Na_2MoO_4(l)$, H_R, may be estimated from the enthalpy of solution of $Na_2O(l)$ in the Na_2O–MoO_3 melt obtained in this study and the measurements made by Navrotsky and Kleppa. There are four sets of data in Fig. 3 showing the temperature dependence of log a_{Na_2O}. Following the Gibbs–Helmholtz equation:

$$H^M_N = \left[\frac{\partial(G^M_N/T)}{\partial(1/T)}\right]_{P,N} = \left[\frac{(\partial R\ln a_{Na_2O})}{\partial(1/T)}\right]_{P,N} \quad (15)$$

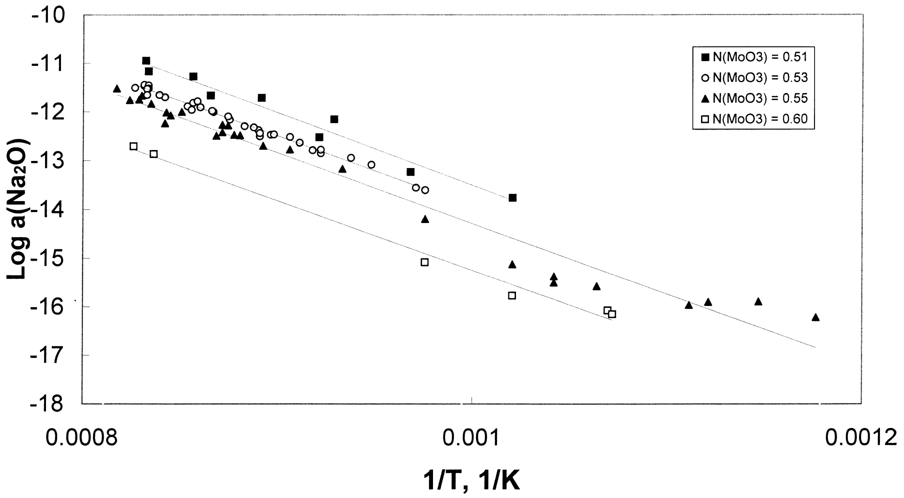

Fig. 3. Temperature dependence of the Na_2O activity in the Na_2O–MoO_3 melt.

Table 2
Enthalpies of solution and calculated H_R in the Na_2O–MoO_3 melt

N_M	H_N^M (kJ/mole)	$H_{M(s)}^M$ (kJ/mole)	H_M^M (kJ/mole)	H_{NM}^M (kJ/mole)	H_R (kJ/mole)
0.51	−284.1	7.32	−39.41	−0.04	−323.6
0.53	−274.4	8.37	−38.36	−0.28	−312.5
0.55	−276.6	10.33	−36.40	−0.59	−312.4
0.60	−272.0	14.35	−32.38	−2.43	−302.0

the enthalpy of solution of $Na_2O(l)$ in the melt, H_N^M, can be obtained from the slope of the lines in Fig. 3. Four H_N^M values corresponding to the melts of $N_M = 0.51$, 0.53, 0.55 and 0.60, respectively, can be estimated. From these estimates and data of Navrotsky and Kleppa, four H_R values can be calculated from Eq. (13). Table 2 summarizes the enthalpies of solution and the calculated H_R values for the four melt compositions.

The average H_R value from these data is −312.6 kJ/mole with a standard deviation of 7.6 kJ/mole. A similar reaction between Na_2O and WO_3 was found to be −341 kJ/mole [18]. Knowing the similarity between WO_3 and MoO_3, we judge that this estimate is reasonable. Using this value and enthalpy of solution data from Navrotsky and Kleppa, a new set of H_N^M for the entire Na_2O–MoO_3 melt can be estimated. Fig. 4 shows the calculated results along with the experimentally obtained estimate from this study. The agreement is good. The enthalpy of solution of Na_2O in the melt may be represented as a function of the melt composition as following:

$$H_N^M = -532.8N_M^2 + 499.37N_M - 389.29,\ \text{kJ/mole} \tag{16}$$

Combining Eq. (11), Eq. (15) and Eq. (16), an equation representing the activity of Na_2O in molten Na_2O–MoO_3 solution can be expressed as:

$$\log a_{Na_2O} = 16.03N_M^2 - 30.18N_M + 12.16 + (-27\,830N_M^2 + 26\,084N_M - 20\,334)/T \tag{17}$$

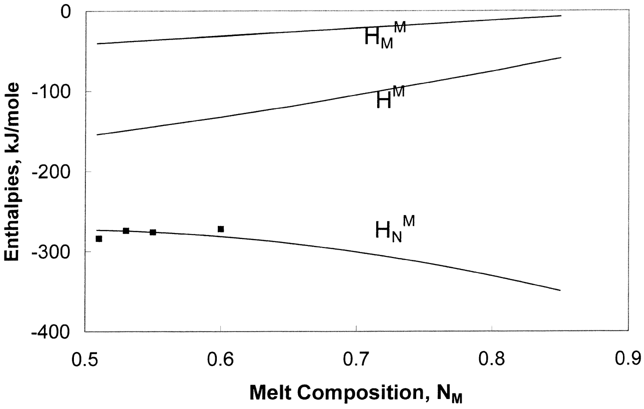

Fig. 4. Enthalpies of solution in the Na_2O–MoO_3 melt.

It is to be noted that experimentally, the EMF technique is good for determining the partial molar free energy of a component in a solution whereas the calorimetric technique would provide accurate measurements on the enthalpy. Thus in this study, the temperature dependence of the Na_2O activity is only used to obtain the enthalpy of reaction, H_R, between $Na_2O(l)$ and $MoO_3(l)$ to form $Na_2MoO_4(l)$. The calorimetric data determined by Navrotsky and Kleppa were used to obtain the enthalpy of solution of $Na_2O(l)$, H_N^M, in the melt.

3.3. The activity of MoO_3

The activity of MoO_3 in the melt may be evaluated from the Na_2O activity equation shown above and the Na_2O–MoO_3 phase diagram following the Gibbs–Duhem equation. The phase diagram of MoO_3 used in this study is from Caillet [9]. The composition of the melt in equilibrium with solid MoO_3 may be retrieved from the liquidus curve of the phase diagram. The activity of MoO_3 at these compositions is unity at corresponding temperatures reference to the pure solid MoO_3 standard state. However, since we are interested in the thermodynamic properties of the melt both below and above the melting point of MoO_3, it is desirable to express the MoO_3 activity reference to only one standard state. In this study, we select pure liquid MoO_3 at all temperatures as the standard state. The activity of MoO_3 of the melts in equilibrium with pure solid MoO_3 may be calculated from the Gibbs free energy of melting of MoO_3. From the JANAF Tables [21], the enthalpy of melting of MoO_3 is 48.53±4.18 kJ/mole at the melting point, 1074 K. From this value, the standard free energy of melting of $MoO_3(s)$ can be obtained as:

$$MoO_3(s) = MoO_3(l);$$

$$\Delta G^0_{m,\,MoO_3} = 48\,530 - 45.2T;\ \text{J/mole} \tag{18}$$

Thus, the free energy of mixing for MoO_3 at the liquidus composition and temperature may be calculated as:

$$G_M^M = -\Delta G^0_{m,\,MoO_3} = RT \ln a_{MoO_3} \tag{19}$$

At 980 K, the melt at the liquidus has a composition of $N_M = 0.916$ from the phase diagram obtained by Caillet [9]. From Eqs. (18) and (19), the activity of MoO_3 at 980 K and $N_M = 0.916$ can be calculated, and $\log a_{MoO_3} = -0.226$. This value is used as the initial point for the Gibbs–Duhem integration to calculate the MoO_3 activity of the melt for the entire molten region. The MoO_3 activity calculated at 980 K may be represented as:

$$\log a_{MoO_3} = -12.37N_M^2 + 21.17N_M + 8.20 \log N_M - 8.93 \tag{20}$$

Knowing the activities of Na_2O and MoO_3 in the melt,

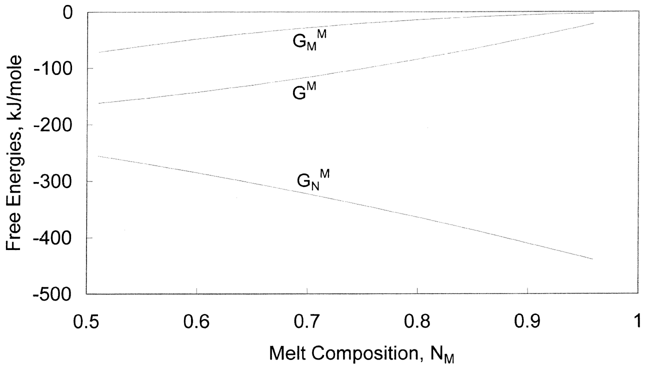

Fig. 5. Gibbs free energies of the Na_2O–MoO_3 melt at 980 K.

the partial molar free energies of Na_2O and MoO_3 can be calculated. The mole fraction sum of the partial free energies gives the integral free energy of the melt. These quantities were calculated for the Na_2O–MoO_3 melt at 980 K and are plotted in Fig. 5.

4. Conclusions

Thermochemistry of the Na_2O–MoO_3 system has been studied using a high temperature EMF cell with Na, β-alumina as the solid state electrolyte. The activity of Na_2O in the Na_2O–MoO_3 melt was determined. Based on the measured results, the following observations can be concluded:

(1) The activity of Na_2O in the entire melt of Na_2O–MoO_3 can be expressed as a simple equation as a function of the melt composition and the temperature.

(2) The MoO_3 activity in the Na_2O–MoO_3 melt has be calculated using the Gibbs–Duhem equation.

(3) Using results from this study and measurements made by Navrotsky and Kleppa, the enthalpy of solution of Na_2O in the melt has been calculated and expressed as a second-order polynomial function of the melt composition.

(4) The enthalpy of reaction between $Na_2O(l)$ and $MoO_3(l)$ to become $Na_2MoO_4(l)$ was estimated to be -312.6 kJ/mole at 970 K.

(5) Partial molar free energies of Na_2O and MoO_3 as well as the integral molar free energy of the melt are obtained for the melt at 980 K.

References

[1] W.T. Reid, R.C. Corey, B.J. Cross, Trans. ASME 67 (1945) 279.
[2] C. Sykes, H.T. Shirley, in: Special Report No. 43, Iron and Steel Institute, 1952, p. 153.
[3] E.L. Simons, G.V. Browning, H.A. Liebhafsky, Corrosion 11 (1955) 505.
[4] A.U. Seybolt, Trans. TMS-AIME 242 (1968) 1955–1961.
[5] N.S. Bornstein, M.A. DeCrescente, Trans. TMS-AIME 245 (1969) 1947–1952.
[6] N.S. Bornstein, M.A. DeCrescente, Metall. Trans. 2 (1971) 2875–2883.
[7] J.A. Goebel, F.S. Pettit, G.W. Goward, Metall. Trans. 4 (1973) 261–278.
[8] V.F. Hoermann, Z. Anorg. Allg. Chem. 177 (1928) 145–149.
[9] P. Caillet, Bull. Soc. Chim. Fr. No. 12 (1967) 4751–4758.
[10] M.F. Koehler, L.B. Pankratz, R.B. Arany, US Bur. Mines, Rep. Invest. 1961, p. 5973.
[11] W.W. Weller, E.G. King, US Bur. Mines, Rep. Invest., 1962, p. 7147.
[12] A. Navrotsky, O.J. Kleppa, Inorg. Chem. 6 (1967) 2119–2126.
[13] J.L. Holm, O.J. Kleppa, Am. Mineral. 51 (1966) 1608.
[14] A. Navrotsky, O.J. Kleppa, J. Inorg. Nucl. Chem. 30 (1968) 479.
[15] A. Navrotsky, O.J. Kleppa, Inorg. Chem. 8 (1969) 756.
[16] F. Muller, O.J. Kleppa, J. Inorg. Nucl. Chem. 35 (1973) 2673.
[17] W.W. Liang, J.F. Elliott, J. Electrochem. Soc. 123 (1976) 617–621.
[18] R.Y. Lin, J.F. Elliott, Metall. Trans. 14A (1983) 1713–1720.
[19] C.T. Huang, R.Y. Lin, Metall. Trans. 20B (1989) 197–204.
[20] R.Y. Lin, Physical Chemistry of Some Molten Salts, Doctoral Thesis, MIT, February 1980.
[21] JANAF Thermochemical Tables, 2nd Edition, NSRDS-NBS 37, US Department of Commerce, 1970, Supplement to Date, Dow Chemical, MI.
[22] J.P. Hager, J.F. Elliott, Trans. TMS-AIME 239 (1967) 513.
[23] O. Kubaschewski, C.B. Alcock, in: Metallurgical Thermochemistry, 5th Edition, Pergamon Press, Oxford, 1979, pp. 298–331.